

Effective Biosorption of Phosphate from Water Using Fe(III)-Loaded Pomegranate Peel



This work is licensed under a Creative Commons Attribution 4.0 International License

N. Bashyal,^a S. Aryal,^a R. Rai,^a P. C. Lohani,^b
S. K. Gautam,^a M. R. Pokhrel,^c and B. R. Poudel^{a,c,*}

^aDepartment of Chemistry, Tri-Chandra Multiple Campus, Tribhuvan University, Kathmandu, Nepal

^bDepartment of Chemistry, Amrit Campus, Tribhuvan University, Kathmandu, Nepal

^cCentral Department of Chemistry, Institute of Science and Technology, Tribhuvan University, Kathmandu, Nepal

doi: <https://doi.org/10.15255/CABEQ.2022.2174>

Original scientific paper
Received: December 30, 2022
Accepted: May 24, 2023

Removal of phosphate from wastewater is necessary for the safety of public health and environmental protection. The present study used an easily available and affordable biosorbent obtained from the pomegranate peel for the excision of phosphate from water. The biosorption behavior of raw pomegranate peel powder (RPGPP) was found negligible. The RPGPP was further saponified with $\text{Ca}(\text{OH})_2$, followed by Fe(III) loading to obtain Fe(III)-loaded pomegranate peels (Fe(III)-PGPP), which was then employed for the phosphate uptake. Fourier transform infrared spectroscopy (FTIR), energy dispersive X-ray (EDX) spectroscopy, scanning electron microscopy (SEM), and X-ray diffraction (XRD) were used to characterize the biosorbent. The batch adsorption test was used to evaluate the adsorption viability of biosorbents for removing phosphate from aqueous solution. Fe(III)-PGPP was determined to have a pH_{PZC} of 5.40. The experimental data were best explained by the Langmuir isotherm and pseudo-second-order kinetic model. Fe(III)-PGPP had the largest phosphate biosorption capacity of 99.30 mg g^{-1} at the optimum pH of 3.0 and 2.5 hours of contact time. From the results obtained, Fe(III)-PGPP adsorbent can be regarded as an effective and cost-efficient material for the treatment of phosphate-anion-contaminated water.

Keywords

wastewater treatment, phosphate, biomass, pomegranate peel, biosorbent

Introduction

Phosphorus is the ninth most abundant element in terms of the percentage of Earth's crustal mass¹. In its trivalent state, it is chemically unstable and is prone to oxidize to the pentavalent state. Phosphorus is seldom found in free state in nature; instead, it is mostly found as oxo-anions, such as the compound phosphate². Plants and animals cannot thrive without this element, as DNA, RNA, ATP, phospholipid, bones, and teeth have phosphorous in the form of phosphate as the key component^{3,4}. Also, it is an important material for many industries, especially in water treatment, fertilizer, water softening, detergents, flame retardants, corrosion inhibitors, paints, foods, drinks, medicine and in a variety of other industries⁵. Although phosphorous is an integral element for living organisms in trace quantities, a higher concentration could weaken the natural ecosystem and quality of water, which results in eu-

trophication⁶. Phosphate squeezing off into surface water can disturb the aquatic environment and deplete the dissolved oxygen level thus exhausting the water quality⁷. As a result, highly effective aquatic phosphate removal has drawn worldwide attention, and has become more important in water treatment⁸. The phosphorous concentration in streams or other flowing water should not surpass 0.10 mg L^{-1} ⁹.

For its removal from water, multiple techniques have been developed, including crystallization¹⁰, chemical precipitation¹¹, membrane separation¹², and ion exchange and biosorption^{13–16}. Ion exchange and biosorption is the most promising method due to its high efficiency, ease of biosorption, and minimum chemical and biological sludge⁸. Phosphate precipitation is a typical extraction procedure that requires the addition of a coagulant to the inorganic form of phosphate. The treatment plant high expenses and insufficient refining of smaller quantities of phosphorous from water are two major drawbacks of this method^{17–19}. Cation exchange resin loaded with high valent metal ions (eg. Fe^{3+} , Zr^{4+} ,

*Corresponding author: Bhoj Raj Poudel, ORCID: <https://orcid.org/0000-0001-7134-5506>, E-mail: bhoj.poudel@trc.tu.edu.np

Al³⁺, etc) with high affinity for the anionic species has been proposed for the efficient removal of anionic species, such as arsenic and phosphorous². Because of its simplicity and effectiveness, metal loading is frequently used despite expensive studies on the removal of phosphate utilizing metal-loaded agricultural waste adsorbents, but its practical applicability remains restricted. This is because biosorbent stability and reusability have often gained less attention than their biosorption and desorption capacities²⁰.

To isolate phosphate, various multivalent metals on agricultural waste or byproducts have been developed, including Zr(IV)-loaded orange waste gel⁷, Fe(III)- and Al(III)-loaded skin split waste²¹, Zr(IV)-loaded okara²², cross-linked Ce(III)-loaded alginate bead juice²³, activated rice husk, and fruit juice residue²⁴, Zr(IV)-loaded watermelon waste⁴. Pomegranate peel, a byproduct of the pomegranate juice industry is an understudied substance that has the potential to be an effective biosorbent for eliminating harmful pollutants from the aquatic environment²⁵. The pomegranate peel accounts for up to 30 % of the overall weight of the fruit. Despite this, it is usually discharged as waste debris and is readily affordable at a very reasonable cost or for free²⁶. As an effective biosorbent, it might be modified with hydroxyl, carboxyl, and carbonyl functional groups found in the cellulose/hemicellulose, pectin, and lignin components. It contains roughly 10 %–15 % pectin, making it a good natural pectin source²⁷. As a result, it may have the potential to be used as bio-adsorbent.

The retention of phosphate utilizing biowaste such as pomegranate peel, on the other hand, has received far less attention. Although the raw pomegranate peel has been applied as a biosorbent for the segregation of several impurities⁴³, it is necessary to remodel the raw biomass to attain superior phosphate remediation efficiency. Pomegranate peel is used as a bio-adsorbent by loading it with Zr(IV) ions for the removal of phosphate ions²⁷. To the best of our knowledge, studies on the biosorption of phosphate using Fe(III)-loaded saponified pomegranate peel powder have not as yet been conducted. Thus, the application of Fe(III)-loaded pomegranate peel as a bio-adsorbent for the removal of phosphate ions from an aqueous medium is the novelty of this study.

The objectives of the study were (1) to make a novel phosphate anion exchanger out of Fe(III)-loaded saponified pomegranate peel (Fe(III)-PGPP), and to characterize the adsorbent that was made; (2) using batch techniques, to evaluate the sorption performance of Fe(III)-PGPP for phosphate removal from polluted water; (3) to study sorption isotherms, kinetics, and the influence of competing ions on

phosphate removal; and (4) based on the study's findings, to investigate the underlying mechanism of phosphate biosorption on Fe(III)-PGPP.

Experimental

Reagents

Analytical-grade reagents were used without further purification. Ferric chloride hexahydrate (FeCl₃·6H₂O), calcium hydroxide (Ca(OH)₂), and potassium dihydrogen phosphate (KH₂PO₄) were purchased from Sigma Aldrich, New Delhi, India. All working solutions were made in deionized water. The stock solution of phosphate (1000 mg L⁻¹) was made by the dissolution of 1.43 g of KH₂PO₄ in 1000 mL water. The stock solution was then diluted for batch studies of varying concentrations from 10 – 900 mg L⁻¹. Solutions of pH values extending from 1 to 7 were employed. 0.1 M sodium hydroxide (NaOH) and 0.1 M hydrochloric acid (HCl) solutions were used for the pH adjustments.

Preparation of biosorbent

Pomegranate peel was collected from several fruit shops in Kirtipur, Kathmandu. It was washed with water and exposed to sunshine for about a week to remove any undesirable particles. To obtain precise particle size, it was cut into smaller pieces, then ground in a mill, and sieved to 180 µm mesh. It was then rinsed in distilled water to eliminate any water-soluble components before being dried for 24 hours at 60 °C and designated as RPGPP. For the saponification process, roughly 20 g of RPGPP was treated with a saturated solution of Ca(OH)₂ in a 250-mL conical flask and agitated for about 24 hours at 200 rpm. This was then rinsed with water until it reached a neutral pH and dried in an oven (Asian Oven 14) for about 24 hours and was designated as SPGPP. Furthermore, about 10 g of SPGPP was treated with 0.25 M FeCl₃·6H₂O solution and agitated using a shaker (Flask Shaker: Stuart Scientific SFI) at 120 rpm for 24 hours²⁰. It was then washed until it reached a neutral pH and oven-dried at 60 °C. The powder thus obtained was designated as Fe(III)-PGPP, and was weighed and used for batch biosorption studies.

Characterization

FTIR spectroscopy was used to examine the surface functional group variation in raw, saponified, and phosphate-loaded adsorbent on IR-Affinity-1S SHIMADZU spectrometer (Kyoto, Japan). FTIR spectra of all samples were recorded using the ATR (attenuated total reflection) method in the spectral range of 4000 to 400 cm⁻¹ wavenumber

range with a resolution of 4 cm^{-1} , and the number of scans was 32. The morphology and elemental mapping of as-prepared biosorbent were investigated using field emission scanning electron microscopy (FE-SEM; JEOL, JSM-6701 F, Japan) fitted with an energy dispersive X-ray (EDX) spectrometer. X-ray diffraction (XRD) was used to identify crystallographic structures with a computer-controlled X-ray diffractometer (Rigaku Co., Japan) with $\text{Cu K}\alpha$ ($\lambda = 1.54056 \text{ \AA}$) radiation. The pH_{PZC} of the adsorbent was measured using the pH drift method. For this, NaCl solutions of concentrations 0.01 M, 0.05 M, and 0.1 M were prepared. The initial pHs of solutions were maintained at pH 2, 3, 4, 5, 6, 7, 8, and 9 using HCl and NaOH solutions. An amount of 25 mL of pH-adjusted 0.01 M NaCl solutions with 25 mg of Fe(III)-loaded adsorbent was shaken in a shaker for 24 hours. The equilibrated solutions were filtered, and the final pH of filtrates was analyzed using a pH meter (Deluxe pH meter, Max Electronics, India). The difference in pH was calculated, and this difference in pH vs initial pH was plotted. A similar procedure was repeated for 0.05 M and 0.1 M NaCl solutions.

Batch biosorption experiments

The biosorption behavior of phosphate on pomegranate peel powder (RPGPP) and Fe(III)-PGPP was investigated using batch biosorption experiments. The effect of several operational factors, such as pH, biosorbent dosage, contact time, and starting phosphate concentration on Fe(III)-PGPP was explored to determine the process optimal conditions.

Influence of pH

Batch pH investigations were carried out to study the impact of solution pH on the biosorption process. An amount of 25 mL of each phosphate solution (20 mg L^{-1}) of pH 1 to 8 were mixed with 25 mg of biosorbents (RPGPP and Fe(III)-PGPP), and the mixtures were agitated for 24 hours to achieve equilibrium. 0.1 M NaOH and 0.1 M HCl solutions were employed for the pH adjustments.

Biosorption kinetics studies

Furthermore, by mixing 25 mg of biosorbent with 25 mL of 20 mg L^{-1} phosphate solution at optimal pH of 3.0, the pH at which the phosphate adsorption was maximum, the kinetics of phosphate on Fe(III)-PGPP were investigated. Biosorption trials at various periods (10 min, 20 min, 30 min, 40 min, 50 min, 60 min, 75 min, 100 min, 120 min, 150 min, 200 min, 250 min, and 300 min) were investigated. Throughout the experiment, the pH was maintained at 3.0. Each sample from the container

was promptly filtered using a Whatman filter paper after the required contact times, and the phosphate content at equilibrium was evaluated.

The pseudo-1st-order and pseudo-2nd-order models, Eq. (1) and Eq. (2) were fitted to the kinetic data using nonlinear equations, respectively. To obtain the linear versions of Eqs. (3) and (4), the nonlinear equations had to be reorganized as follows²⁵:

$$q_t = q_e (1 - e^{-k_1 t}) \quad (1)$$

$$\frac{q k t}{q k t} \quad (2)$$

$$\log (q_e - q_t) = \log q_e - \frac{k_1}{2.303} t \quad (3)$$

$$\frac{t}{q_t} = \frac{1}{k_2 q_e^2} + \frac{1}{q_e} t \quad (4)$$

where q_e and q_t in mg g^{-1} are the biosorption capacities at equilibrium and at time t , respectively, and k_1 (min^{-1}) and k_2 ($\text{g mg}^{-1} \text{ min}^{-1}$) are the rate constants of pseudo-1st-order and pseudo-2nd-order kinetics, respectively.

Biosorption isotherm studies

The biosorption isotherm and maximum biosorption capabilities of Fe(III)-PGPP biosorbent were investigated by agitating 25 mg of Fe(III)-PGPP with 25 mL of phosphate solution at optimal pH of 3.0 in different concentration ranges (10 mg L^{-1} to 1000 mg L^{-1}) for 24 hours to achieve equilibrium. To determine equilibrium phosphate concentrations, all the samples were filtered, and analyzed models of Langmuir and Freundlich isotherm were used to illustrate phosphate sorption behavior. Using the Langmuir isotherm model, the adsorbed species have no substantial interaction with each other since the biosorption sites are evenly distributed^{29,30}. Eq. (5) explains the Langmuir model³¹.

$$q_e = \frac{q_m b c_e}{1 + b c_e} \quad (5)$$

It can be expressed linearly according to Eq. (6) as:

$$\frac{c_e}{q_e} = \frac{1}{q_m b} + \frac{c_e}{q_m} \quad (6)$$

where c_e (mg L^{-1}) is the equilibrium concentration of phosphate, q_e (mg g^{-1}) is the equilibrium sorption capacity, q_m (mg g^{-1}) is the maximal sorption capacity corresponding to complete monolayer coverage, and b (L mg^{-1}) is the Langmuir equilibrium constant associated with sorption energy.

On a heterogeneous surface, the Freundlich isotherm model predicts multilayer sorption. The Freundlich model is described by Eq. (7)³².

$$q_e = K_F (c_e)^{1/n} \quad (7)$$

It can be expressed according to Eq. (8) in the linear form as:

$$\log q_e = \log K_F + \frac{1}{n} \log c_e \quad (8)$$

where Freundlich constant K_F [(mg g⁻¹) (L mg⁻¹)^{1/n}] is associated with sorption capacity, and $1/n$ is the dimensionless heterogeneity factor linked with the sorption intensity.

Additionally, a dimensionless separation factor ' R_L ' determines whether or not the biosorption procedure is beneficial²⁹.

$$R_L = \frac{1}{1 + (bc_0)} \quad (9)$$

The Langmuir isotherm is linear at a constant temperature, $R_L > 1$ denotes unfavorable sorption, R_L value between 0 and 1 indicates favorable sorption, and $R_L = 0$ represents irreversible sorption³⁰.

The equations (10) and (11) were used to calculate the percentage of phosphate biosorption and the quantity of phosphate adsorbed per unit weight of biosorbent q_e in mg g⁻¹

$$q_e = \frac{(c_0 - c_e)V}{m} \quad (10)$$

$$A(\%) = \frac{(c_0 - c_e)}{c_0} \cdot 100 \quad (11)$$

where c_0 and c_e (mg L⁻¹) are the starting and equilibrium phosphate concentrations, V is the solution volume, and m (g) is the biosorbent weight.

Analysis of phosphate

The concentration of phosphate ions in test solution before and after adsorption was analyzed by colorimetric method in the presence of ammonium molybdate and potassium antimonyl tartrate using ascorbic acid as reducing agent ($\lambda_{\max} = 880$ nm), with a UV-Visible double beam spectrophotometer (Labtronics, LT-2802, India)³³.

Results and discussion

Characterization of the biosorbents

The pH drift technique was used to determine the pH_{pZC} of the adsorbent. As illustrated in Fig. 1, the point of zero charges (pH_{pZC}) of Fe(III)-PGPP was found to be about 5.40. This suggests Fe(III)-PGPP has no net surface charge at a pH value of 5.40. At $pH > 5.40$, the surface of Fe(III)-PGPP is negatively charged, making anionic species biosorption difficult due to repulsive forces. However, at $pH < 5.40$, the Fe(III)-PGPP surface is positively charged, making the biosorption of anionic species like the phosphate anion easier.

Fig. 2 shows the SEM images of raw, saponified, iron-loaded, and phosphate-adsorbed biosorbents. The bulk of the RPGPP surface was smooth, but there were some shiny patches scattered throughout Fig. 2a, whereas the surface became significantly rougher and uneven following saponification, indicating surface change by chemical treatment Fig. 2b. The Fe(III)-PGPP surface was smoother than RPGPP, indicating that the Fe(III) metal was loaded onto the SPGPP adsorbent Fig. 2c; nevertheless, following phosphate biosorption, the surface became smoother (Fig. 2d).

The EDX spectra of Fe(III)-PGPP following phosphate sorption are shown in Fig. 3. After phosphate biosorption, binding energies of around 0.26 keV, 0.5 keV, 0.6 keV, and 2.0 keV were measured for the peaks corresponding to C, O, Fe, and P. It has been confirmed that the studied biosorbent efficiently absorbed phosphate because of the presence of 0.03 percent P on the Fe(III)-PGPP surface after biosorption. The loaded Fe(III) ions did not leach away during the phosphate biosorption mechanism, as seen by an additional peak in the EDX spectra, and this was subsequently confirmed by surface color mapping, which displayed the elemental distribution (Fig. 3b). The sorption product's EDX color mapping study demonstrated that phosphate biosorption proceeded consistently.

In the FTIR spectra of RPGP (Fig. 4), a broad and strong band at 3317 cm⁻¹ is assigned to the stretching vibration of (-OH) groups of alcohol and carboxylic acid in cellulose, hemicelluloses, pectin, and lignin. This peak widens in the case of Fe-loaded adsorbents indicating the presence of absorbed water molecules. The peak at 2920 cm⁻¹ is due to CH stretching vibration. The peak at 1730 cm⁻¹ is

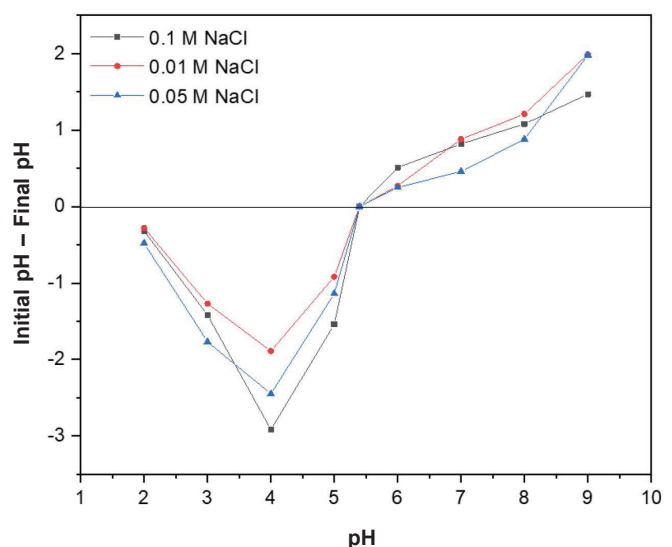


Fig. 1 – Variation of pH of NaCl solution after contact with Fe-PGPP for the determination of pH_{pZC} by pH drift method

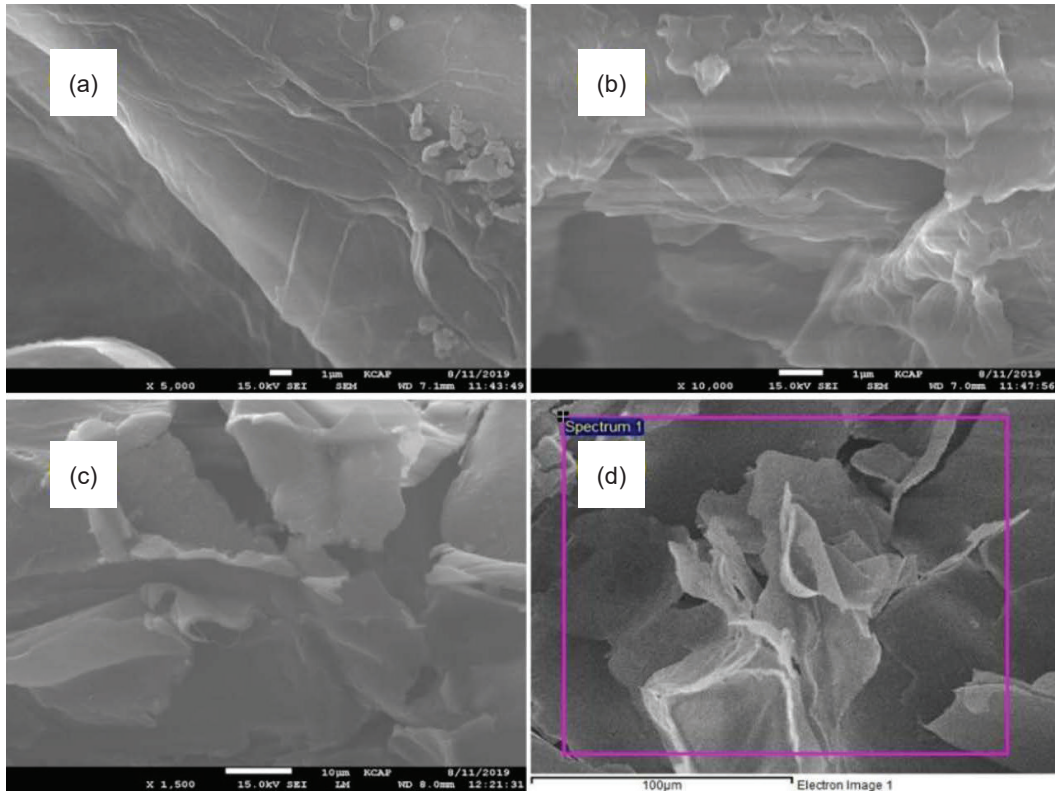


Fig. 2 – SEM images of (a) RGP, (b) SPGP, (c) Fe(III)-PGP without biosorption, and (d) Fe(III)-PGP after phosphate biosorption

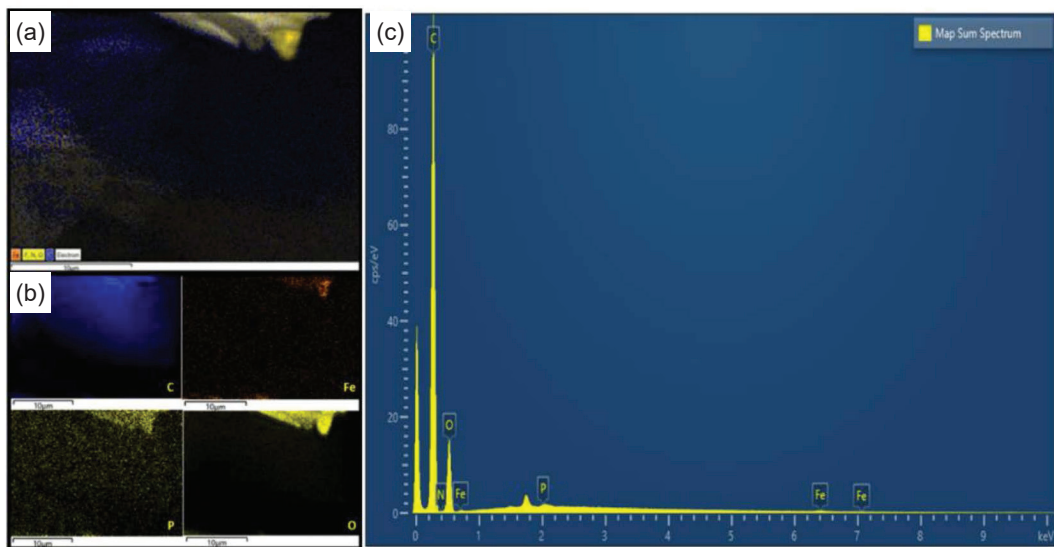


Fig. 3 – (a) EDS layered image, (b) color mapping illustrating the elemental distribution of Fe(III)-PGP after biosorption, (c) EDS spectra of Fe(III)-PGP after phosphate biosorption

assigned to the C=O stretching vibration of the carboxyl group or ester. Two peaks were observed at 1605 cm^{-1} and 1411 cm^{-1} , attributed to the stretching vibration of ionic carboxyl ($-\text{COO}$) groups³⁴. After saponification, the peak at 1728 cm^{-1} disappeared, the peak at 1605 cm^{-1} became more intense,

and a new peak appeared at around 1420 cm^{-1} which was attributed to the existence of the O–Ca bond³⁵. Due to the interchange of high molecular weight metal Fe with Ca during the Fe(III) loading process, the peak changed to a lower frequency area in Fe(III)-PGP.

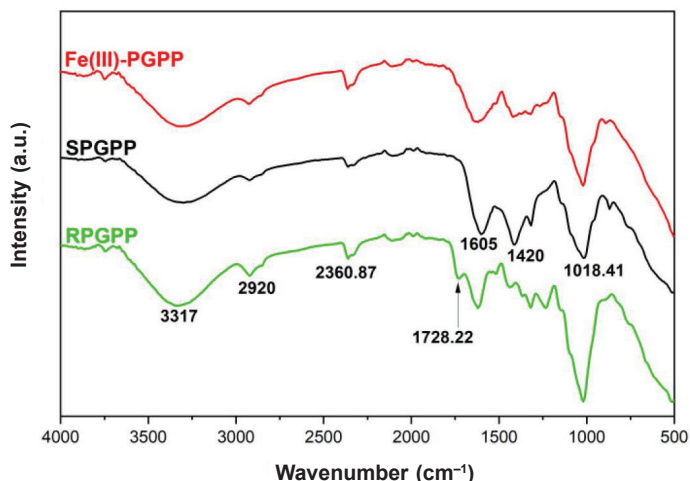


Fig. 4 – FTIR spectra of RPGPP, SPGPP, and Fe(III)-PGPP

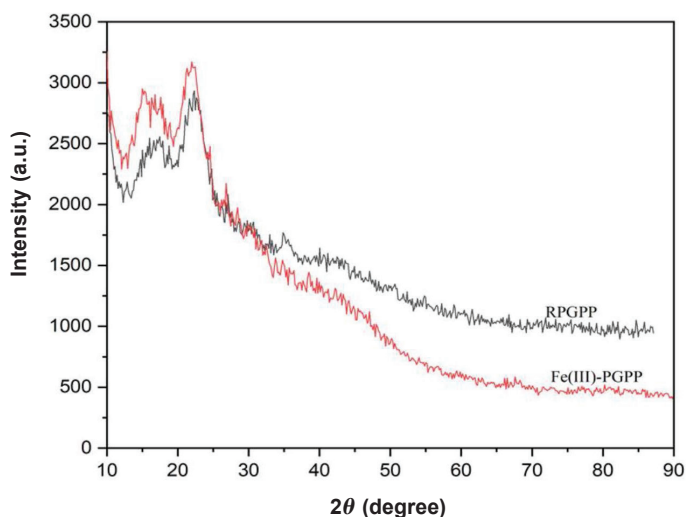


Fig. 5 – XRD pattern of RPGPP and Fe(III)-PGPP

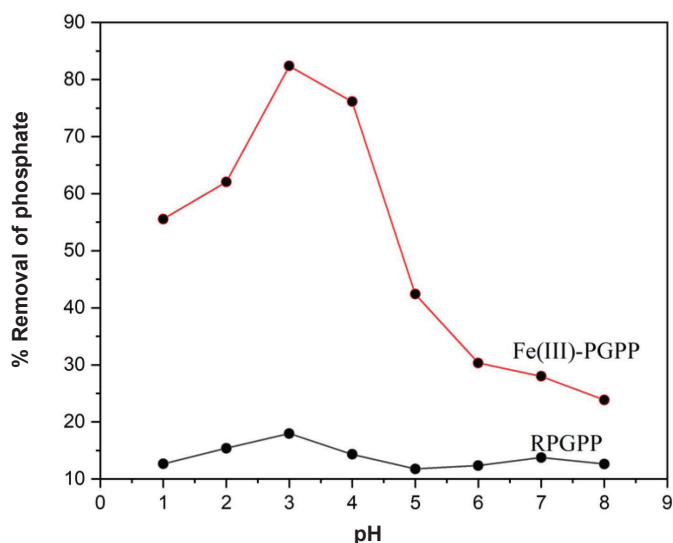


Fig. 6 – Effect of initial pH on the biosorption of phosphate on RPGPP and Fe(III)-PGPP

Fig. 5 shows the XRD patterns used to examine the crystalline nature of RPGPP and Fe(III)-PGPP. RPGPP has a prominent peak at $2\theta = 9^\circ$ and multiple weak and dispersed peaks at higher angles, according to its XRD pattern. RPGPP has both amorphous and crystalline sections, implying that it has both amorphous and crystalline regions. According to the structure of the material, crystallinity can be affected substantially by its content of the three main types of cellophane (lignin/hemicelluloses/cellulose). In Fe(III)-PGPP, the prominent peak at $2\theta = 9^\circ$ stays unaltered, indicating that the modification process occurs solely in amorphous zone³⁶. The amorphous form of bio-adsorbents contributes to their high biosorption capacity^{19,37}.

Batch experiment

Effect of initial pH

In the case of RPGPP adsorbents, phosphate biosorption is negligible (less than 20 %) at all pH levels examined. The phosphate biosorption utilizing the Fe(III)-loaded adsorbent, on the other hand, improved dramatically, possibly due to the formation of additional active sites for the phosphate anion by Fe(III) loading. In comparison to Fe(III)-PGPP, RPGPP's biosorption capacity appears to be minimal. As a result, RPGPP as a biosorbent was ignored in ongoing studies.

According to the results presented in Fig. 6, increasing the pH of the solution from 1.0 to 3.0 enhanced phosphate biosorption from 55.56 % to 82.36 %, then it was shown to decline with a further increase in pH. At a pH of 3.0, the highest biosorption occurred.

Phosphate can be found in a variety of ionic species based on the pH of the aquatic medium ($pK_1 = 2.15$, $pK_2 = 7.20$, $pK_3 = 12.33$)⁴. It occurs in the form of its neutral species at pH below 2, which is difficult to adsorb onto active sites, resulting in a reduction in phosphate absorption capacity at pH below 2.0. As the majority of phosphate residues are in the form of the monovalent anion ($H_2PO_4^-$) at optimal pH, the biosorption of this monovalent species of phosphate anion is favored by using a ligand exchange process to replace the hydroxyl ligand (monovalent ligand), as indicated in Fig. 7. The concentration of competing $-OH$ ions increased when the pH was raised above the optimal pH, resulting in a fall in percentage biosorption.

Even at extremely low concentrations, Fe(III) ions tend to be extensively polymerized and hydrolyzed, comprising numerous hydroxyl ions as well as water molecules coupled to Fe(III) ion under-hydrated state. The ligand exchange process between these OH^- or H_2O molecules and phosphorus species occurs⁷. Biosorption occurs through the ex-

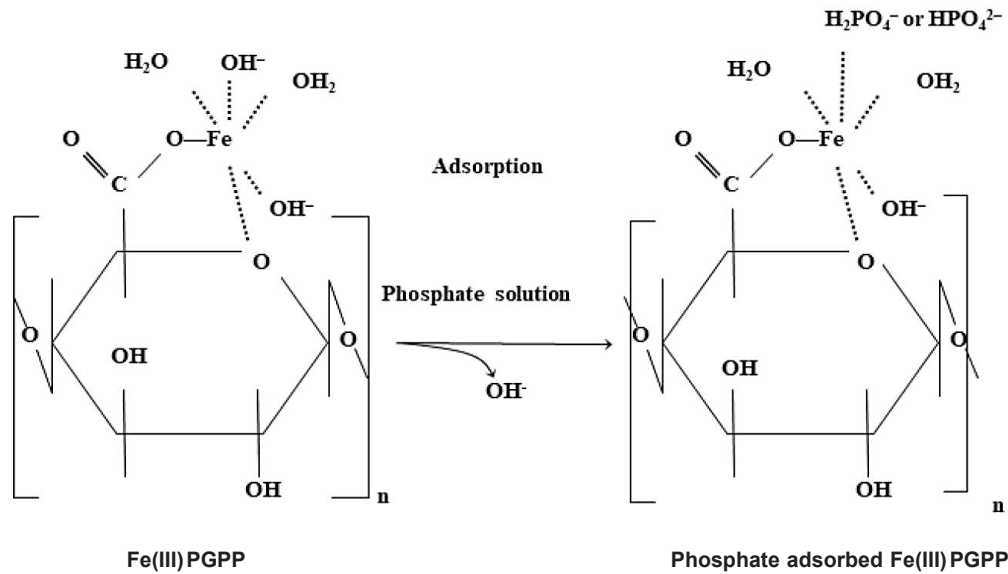


Fig. 7 – Inferred mechanism of ligand exchange for phosphate biosorption onto Fe(III)-PGPP

change of anions with OH⁻ ions associated with metal in the coordination sphere, as evidenced by the increase in initial pH following equilibration for those pH levels where biosorption is favorable. As a result, the ligand exchange mechanism is likely to be the most compelling for phosphate biosorption^{4,17}. Similar type of biosorption behavior was observed for the adsorption of phosphate ions onto watermelon waste loaded with Zr(IV).

Effect of initial concentration and isotherm modeling

Using 25 mg Fe(III)-PGPP, at optimal pH, the impact of starting phosphate concentrations (10–1000 mg L⁻¹) was investigated, and the results are shown in Fig. 8. The result showed that phosphate biosorption increased with phosphate content initially. This might be attributed to a reduction in bio-

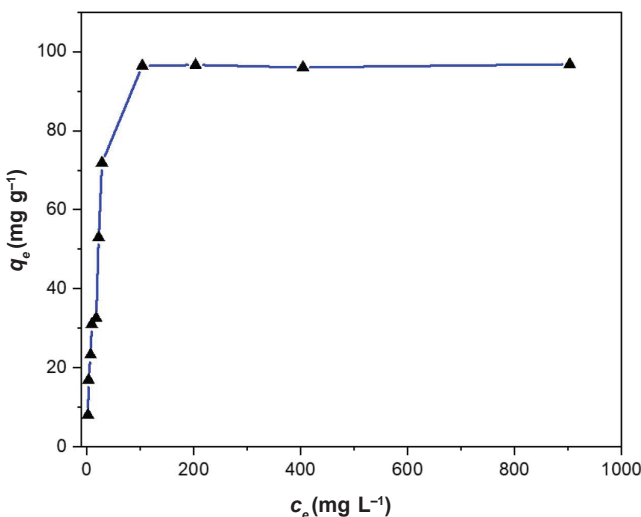


Fig. 8 – Biosorption isotherm of phosphate onto Fe(III)-PGPP

sorption sites, which would increase phosphate biosorption. Phosphate removal is quicker at low concentrations than at high concentrations, implying that Fe(III)-PGPP is acceptable for phosphate removal in aqueous solutions at low concentrations¹⁶.

The Langmuir and Freundlich isotherm models were used to investigate the mechanism of phosphate biosorption onto Fe(III)-PGPP. The phosphate biosorption offers a linear connection with the Langmuir and Freundlich isotherm models, as shown in Fig. 9, from which the adsorbent’s isotherm parameters were calculated as shown in Table 1.

The correlation coefficient (*R*²) values for Langmuir isotherms were reported to be higher than those for Freundlich isotherms, indicating that the Langmuir isotherm model suits the biosorption model better than the Freundlich isotherm model. This signifies monolayer biosorption and uniform allotment of the active spot on the adsorbent surface. The maximum biosorption capacity of Fe(III)-PGPP was calculated using the Langmuir isotherm model and found to be 99.30 mg g⁻¹. The quantity

Table 1 – Isotherms parameters determined for the biosorption of phosphate onto Fe(III)-PGPP

	Parameter	Value
Langmuir isotherm	<i>q</i> _{max} (mg g ⁻¹)	99.30
	<i>b</i> (L mg ⁻¹)	0.057
	<i>R</i> ²	0.9980
Freundlich isotherm	<i>K</i> _{<i>F</i>} (mg g ⁻¹) (L mg ⁻¹) ^{1/<i>n</i>}	11.49
	1/ <i>n</i>	0.658
	<i>R</i> ²	0.8287

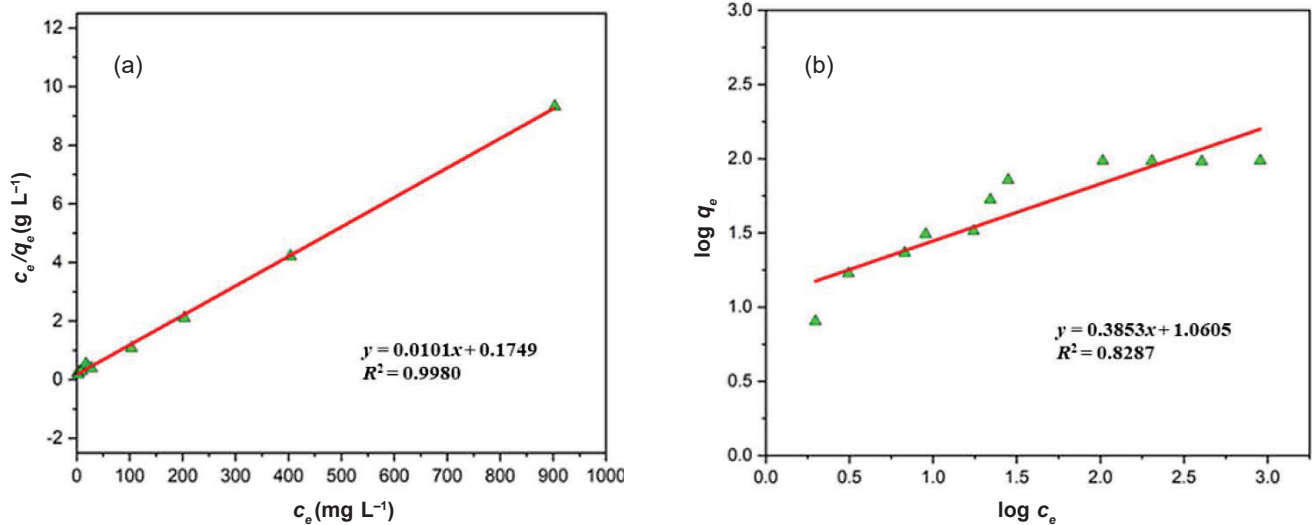


Fig. 9 – (a) Langmuir biosorption isotherm, and (b) Freundlich biosorption isotherm for the biosorption of phosphate on Fe(III)-PGPP at pH 3.0

of phosphate absorbable per unit mass of adsorbent to produce a full monolayer is the maximal biosorption capacity. This result of $q_{\max} = 99.30 \text{ mg g}^{-1}$ is quite like the experimental value of 96.8 mg g^{-1} , which was acquired directly by absorbance measurement. The maximum biosorption capacity of Fe(III)-PGPP for phosphate is superior or analogous to that of different biosorbents reported in past research^{2,4,7,20,24}. It suggests that Fe(III)-PGPP could serve as an effective and potential anion exchanger for removing phosphate from water.

Effect of contact time and kinetic modeling

By altering the contact duration while keeping the other parameters constant, the effect of contact time was explored. Information about rates of biosorption as a function of time and estimation of optimum contact time for complete saturation of active sites for biosorption was obtained. The equilibrium contact time for phosphate biosorption onto Fe(III)-PGPP was roughly 2 hours and 30 minutes, as shown in Fig. 10. During the early stages of phosphate biosorption, the rate of phosphate biosorption was quite fast. A high biosorption rate is due to the abundance of biosorption sites, which allows a large number of phosphate ions to be initially connected to the adsorbent sites^{24,38}. The rate of phosphate biosorption steadily dropped until it reached equilibrium at 2 hours 30 minutes, after which there was no significant rise in the biosorption rate due to the lack of effective empty sites in the adsorbents.

Pseudo-first-order and pseudo-second-order models were used to investigate the kinetics of phosphate biosorption on Fe(III)-PGPP. The kinetic graphs of both pseudo-first-order and pseudo-second-order models yielded straight lines. To calculate k_1 and k_2 , q_e and R^2 for both models, two autonomous graphs of $\log(q_e - q_t)$ vs t and t/q_t vs t were plotted. Table 2 lists the estimated values of kinetic parameters. Compared to the R^2 of the pseu-

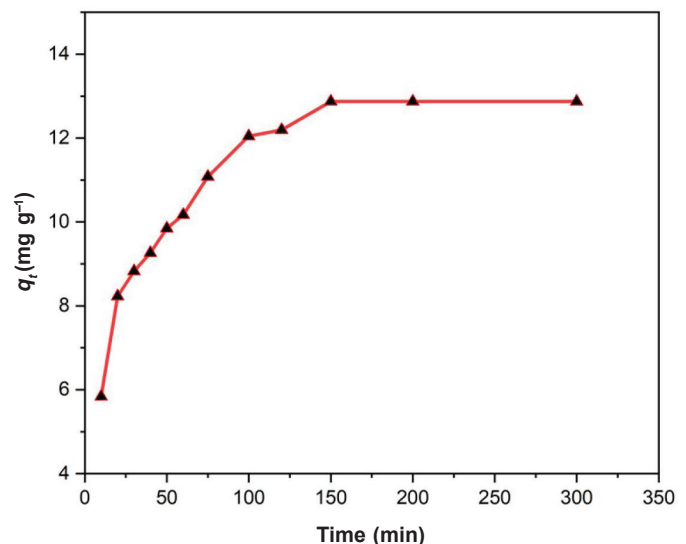


Fig. 10 – Effect of contact time on the biosorption of phosphate onto Fe(III)-PGPP at pH 3.0

Table 2 – Kinetic parameter determined for the biosorption of phosphate onto Fe(III)-RPGPP

Order	R^2	q_e (exp) (mg g ⁻¹)	q_e (cal) (mg g ⁻¹)	k_1 (min ⁻¹)	k_2 (g mg ⁻¹ min ⁻¹)
Pseudo-second-order	0.9500	12.87	12.32	–	$5.35 \cdot 10^{-3}$
Pseudo-first-order	0.9200	12.87	6.99	$1.70 \cdot 10^{-2}$	–

ond-order models yielded straight lines. To calculate k_1 and k_2 , q_e and R^2 for both models, two autonomous graphs of $\log(q_e - q_t)$ vs t and t/q_t vs t were plotted. Table 2 lists the estimated values of kinetic parameters. Compared to the R^2 of the pseu-

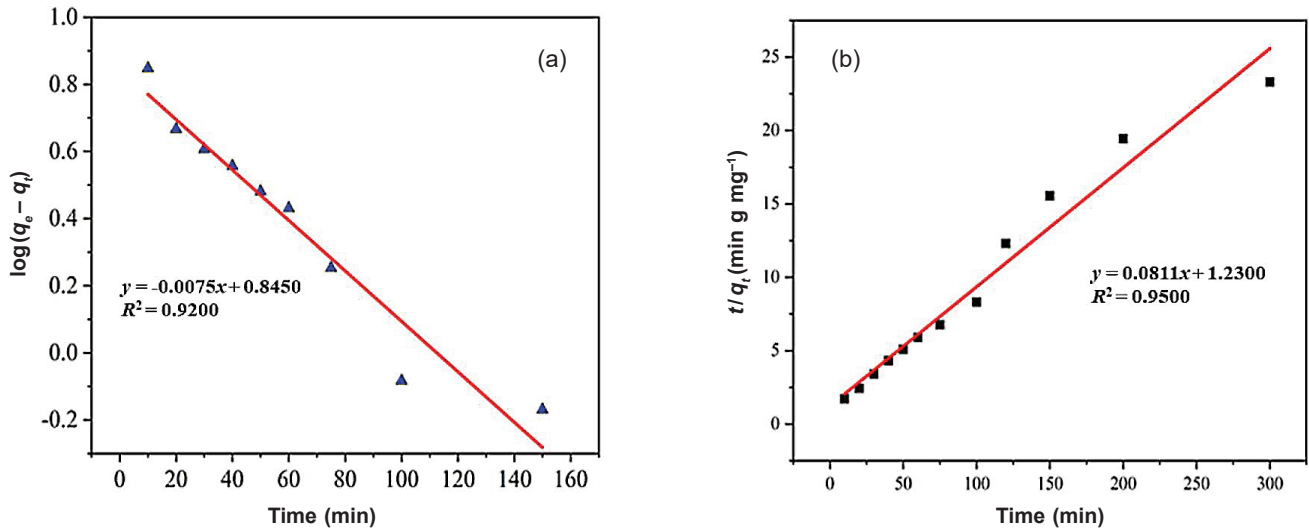


Fig. 11 – (a) Pseudo-first-order kinetic model, and (b) Pseudo-second-order kinetic model for the biosorption of phosphate onto Fe(III)-PGPP at pH 3.0

do-first-order model, that of the pseudo-second-order model (0.95) was closer to unity. Another interesting finding was the close match between the experimental and theoretical equilibrium biosorption capacity of Fe(III)-PGPP in the pseudo-second-order kinetics (q_e (cal) = 12.87 mg g⁻¹). Because the phosphate biosorption processes on Fe(III)-PGPP took place in pseudo-second-order kinetics, it was reasonable to assume that the phosphate biosorption was being fueled by chemisorption. The biosorption nature of phosphate ions onto the investigated PGPP is similar to the biosorption behavior of arsenate ions onto saponified Zr(IV)-loaded pomegranate peel²⁷.

Effect of adsorbent dosage

In general, phosphate removal effectiveness increased when the quantity of Fe(III)-PGPP was increased up to 150 mg, then remained constant as the adsorbent dosage was increased further³⁹. More binding sites for phosphate biosorption and a larger surface area accessible at higher adsorbent doses explained the increased phosphate removal effectiveness^{40–42}. The phosphate removal effectiveness decreases or remains constant when the adsorbent dosage exceeds an optimal level. At greater doses, this might be owing to mass transfer barriers, particle aggregates, and repulsive interactions between binding sites^{44,45}.

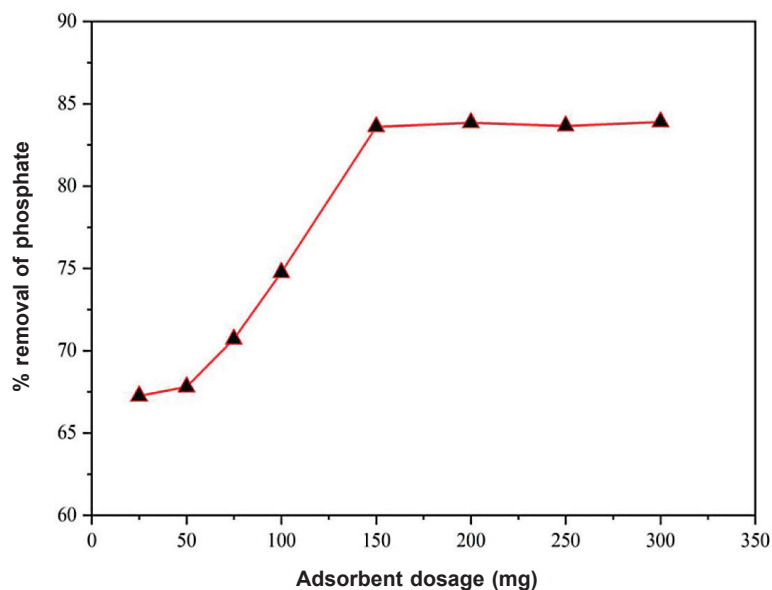


Fig. 12 – Effect of adsorbent dosage on the biosorption of phosphate onto Fe(III)-PGPP at pH 3.0

Conclusions

In this work, the biomass of the pomegranate peel was successfully modified using $\text{Ca}(\text{OH})_2$ followed by loading of Fe(III) ions, resulting in changes in the structural organization of the biosorbent. A series of batch experiments performed to obtain information on the effect of pH, contact time, concentration, and biosorbent dosage confirmed the efficiency of as-prepared biosorbent for phosphate removal. Biosorption of phosphate is substantially pH-dependent, and maximum removal occurred at pH 3.0 for Fe(III)-PGPP. The experimental data were best explained by the Langmuir model of isotherm and the pseudo-second-order model of kinetics. The maximum biosorption capacity of Fe(III)-PGPP for phosphate from Langmuir isotherm modeling was found to be 99.30 mg g^{-1} . As per the findings of the present study, Fe(III)-loaded saponified pomegranate peel powder can be used as an efficient and economic biosorbent for the removal of phosphate from an aqueous environment. From future perspectives, other modifying agents can be investigated, as well as the capacity of the Fe(III)-PGPP explored through a fixed bed column with a view to industrial scale.

References

1. Corbridge, D. E., Phosphorus: Chemistry, Biochemistry and Technology, CRC Press, 2013.
2. Poudel, B. R., Aryal, R. L., Khadka, L. B., Ghimire, K. N., Paudyal, H., Pokhrel, M. R., Development of biomass-based anion exchanger for the removal of trace concentration of phosphate from water, *J. Nepal Chem. Soc.* **41**(1) (2020) 56.
doi: <https://doi.org/10.3126/jncs.v41i1.30488>
3. Song, X., Pan, Y., Wu, Q., Cheng, Z., Ma, W., Phosphate removal from aqueous solutions by biosorption using ferric sludge, *Desalination*. **280** (2011) 384.
doi: [https://doi.org/10.1016/S1001-0742\(13\)60537-9](https://doi.org/10.1016/S1001-0742(13)60537-9)
4. Aryal, R. L., Bhurtel, K. P., Poudel, B. R., Pokhrel, M. R., Paudyal, H., Ghimire, K. N., Sequestration of phosphate from water onto modified watermelon waste loaded with Zr (IV), *Sep. Sci. Technol.* **57**(1) (2022) 70.
doi: <https://doi.org/10.1080/01496395.2021.1884878>
5. Biswas, B. K., Inoue, K., Ghimire, K. N., Ohta, S., Harada, H., Ohta, K., Kawakita, H., The biosorption of phosphate from an aquatic environment using metal-loaded orange waste, *J. Colloid Interface Sci.* **312**(2) (2007) 214.
doi: <https://doi.org/10.1016/j.jcis.2007.03.072>
6. Awual, M. R., Jyo, A., Ihara, T., Seko, N., Tamada, M., Lim, K. T., Enhanced trace phosphate removal from water by zirconium (IV) loaded fibrous adsorbent, *Water Res.* **45**(15) (2011) 4592.
doi: <https://doi.org/10.1016/j.watres.2011.06.009>
7. Biswas, B. K., Inoue, K., Ghimire, K. N., Harada, H., Ohta, K., Kawakita, H., Removal and recovery of phosphorus from water by means of biosorption onto orange waste gel loaded with zirconium, *Bioresour. Technol.* **99**(18) (2008) 8685.
doi: <https://doi.org/10.1016/j.biortech.2008.04.015>
8. Qiu, H., Ni, W., Zhang, H., Chen, K., Yu, J., Fabrication and evaluation of a regenerable HFO-doped agricultural waste for enhanced biosorption affinity towards phosphate, *Sci. Total Environ.* **703** (2020) 135493.
doi: <https://doi.org/10.1016/j.scitotenv.2019.135493>
9. Nakarmi, A., Chandrasekhar, K., Bourdo, S. E., Watanabe, F., Guisbiers, G., Viswanathan, T., Phosphate removal from wastewater using novel renewable resource-based, cerium/manganese oxide-based nanocomposites, *Environ. Sci. Pollut. Res.* **27**(29) (2020) 36688.
doi: <https://doi.org/10.1007/s11356-020-09400-0>
10. Huang, H., Xiao, D., Pang, R., Han, C., Ding, L., Simultaneous removal of nutrients from simulated swine wastewater by biosorption of modified zeolite combined with struvite crystallization, *Chem. Eng. J.* **256** (2014) 431.
doi: <https://doi.org/10.1016/j.cej.2014.07.023>
11. Desmidt, E., Ghyselbrecht, K., Zhang, Y., Pinoy, L., Van der Bruggen, B., Verstraete, W., Meesschaert, B., Global phosphorus scarcity and full-scale P-recovery techniques: A review, *Crit. Rev. Environ. Sci. Technol.* **45**(4) (2015) 336.
doi: <https://doi.org/10.1080/10643389.2013.866531>
12. Lee, G., Modarresi, S., Benjamin, M. M., Efficient phosphorus removal from MBR effluent with heated aluminum oxide particles (HAOPs), *Water Res.* **159** (2019) 274.
doi: <https://doi.org/10.1016/j.watres.2019.05.010>
13. Ortega, A., Oliva, I., Contreras, K. E., González, I., Cruz-Díaz, M. R., Rivero, E. P., Arsenic removal from water by hybrid electro-regenerated anion exchange resin/electrodialysis process, *Sep. Purif. Technol.* **184** (2017) 319.
doi: <https://doi.org/10.1016/j.seppur.2017.04.050>
14. Rai, R., Karki, D. R., Bhattarai, K. P., Pahari, B., Shrestha, N., Adhikari, S., Gautam, S. K., Poudel, B. R., Recent advances in biomass-based waste materials for the removal of chromium (VI) from wastewater: A review, *Amrit Res. J.* **2**(01) (2021) 37.
doi: <https://doi.org/10.3126/arj.v2i01.40736>
15. Poudel, B. R., Ale, D., Aryal, R. L., Ghimire, K. N., Gautam, S. K., Paudyal, H., Pokhrel, M. R., Zirconium modified pomegranate peel for efficient removal of arsenite from water, *BIBECHANA* **19**(1,2) (2022) 1.
doi: <https://doi.org/10.3126/bibechana.v19i1-2.45943>
16. Poudel, B. R., Aryal, R. L., Bhattarai, S., Koirala, A. R., Gautam, S. K., Ghimire, K. N., Pant, B., Park, M., Paudyal, H., Pokhrel, M. R., Agro-waste derived biomass impregnated with TiO_2 as a potential adsorbent for removal of As(III) from water, *Catalysts* **10** (2020) 1125.
doi: <https://doi.org/10.3390/catal10101125>
17. Liu, J., Zhou, Q., Chen, J., Zhang, L., Chang, N., Phosphate biosorption on hydroxyl-iron-lanthanum doped activated carbon fiber, *Chem. Eng. J.* **215** (2013) 859.
doi: <https://doi.org/10.1016/j.cej.2012.11.067>
18. Nakarmi, A., Bourdo, S. E., Ruhl, L., Kanel, S., Nadagouda, M., Alla, P. K., Viswanathan, T., Benign zinc oxide beta-ine-modified biochar nanocomposites for phosphate removal from aqueous solutions, *J. Environ. Manage.* **272** (2020) 111048.
doi: <https://doi.org/10.1016/j.jenvman.2020.111048>
19. Pant, B. D., Neupane, D., Paudel, D. R., Lohani, P. C., Gautam, S. K., Pokhrel, M. R., Poudel, B. R., Efficient biosorption of hexavalent chromium from water by modified arecanut leaf sheath, *Heliyon*. **8**(4) (2022) e09283.
doi: <https://doi.org/10.1016/j.heliyon.2022.e09283>
20. Nguyen, T. A. H., Ngo, H. H., Guo, W. S., Nguyen, T. V., Zhang, J., Liang, S., Nguyen, N. C., A comparative study on different metal loaded soybean milk by-product 'okara' for biosorption of phosphorus from aqueous solution, *Bioresour. Technol.* **169** (2014) 291.
doi: <https://doi.org/10.1016/j.biortech.2014.06.075>

21. Huang, W. Y., Li, D., Liu, Z. Q., Tao, Q., Zhu, Y., Yang, J., Zhang, Y. M., Kinetics, isotherm, thermodynamic, and biosorption mechanism studies of La(OH)₃-modified exfoliated vermiculites as highly efficient phosphate adsorbents, *Chem. Eng. J.* **236** (2014) 191. doi: <https://doi.org/10.1016/j.cej.2013.09.077>
22. Nguyen, T. A. H., Ngo, H. H., Guo, W. S., Zhang, J., Liang, S., Tung, K. L., Feasibility of iron loaded 'okara' for biosorption of phosphorous in aqueous solutions, *Bioresour. Technol.* **150** (2013) 42. doi: <https://doi.org/10.1016/j.biortech.2013.09.133>
23. Yang, Q., Wang, X., Luo, W., Sun, J., Xu, Q., Chen, F., Zeng, G., Effectiveness and mechanisms of phosphate biosorption on iron-modified biochars derived from waste activated sludge, *Bioresour. Technol.* **247** (2018) 537. doi: <https://doi.org/10.1016/j.biortech.2017.09.136>
24. Yadav, D., Kapur, M., Kumar, P., Mondal, M. K., Adsorptive removal of phosphate from aqueous solution using rice husk and fruit juice residue, *Process Saf. and Environ. Prot.* **94** (2015) 402. doi: <https://doi.org/10.1016/j.psep.2014.09.005>
25. Yang, X., Nisar, T., Hou, Y., Gou, X., Sun, L., Guo, Y., Pomegranate peel pectin can be used as an effective emulsifier, *Food Hydrocoll.* **85** (2018) 30. doi: <https://doi.org/10.1016/j.foodhyd.2018.06.042>
26. Ben-Ali, S., Application of raw and modified pomegranate peel for wastewater treatment: A literature overview and analysis, *Int. J. Chem. Eng.* **2021** (2021) 8840907. doi: <https://doi.org/10.1155/2021/8840907>
27. Poudel, B. R., Aryal, R. L., Gautam, S. K., Ghimire, K. N., Paudyal, H., Pokhrel, M. R., Effective remediation of arsenate from contaminated water by zirconium modified pomegranate peel as an anion exchanger, *J. Environ. Chem. Eng.* **9**(6) (2021) 106552. doi: <https://doi.org/10.1016/j.jece.2021.106552>
28. Blanchard, G., Maunaye, M., Martin, G., Removal of heavy metals from waters by means of natural zeolites, *Water Res.* **18**(12) (1984) 1501. doi: [http://doi.org/10.1016/0043-1354\(84\)90124-6](http://doi.org/10.1016/0043-1354(84)90124-6)
29. Wang, J., Guo, X., Biosorption kinetic models: Physical meanings, applications, and solving methods, *J. Hazard. Mater.* **390** (2020) 122156. doi: <https://doi.org/10.1016/j.jhazmat.2020.122156>
30. Al-Ghouti, M. A., Da'ana, D. A., Guidelines for the use and interpretation of biosorption isotherm models: A review, *J. Hazard. Mater.* **393** (2020) 122383. doi: <https://doi.org/10.1016/j.jhazmat.2020.122383>
31. Langmuir, I., The constitution and fundamental properties of solids and liquids, *J. Am. Chem. Soc.* **38** (1916) 2221.
32. Freundlich, H. M. F., Over the biosorption in solution, *J. Phys. Chem.* **57** (1906) 385.
33. Nagul, E. A., McKelvie, I. D., Worsfold, P., Koleva, S. D., The molybdenum blue reaction for the determination of orthophosphate revisited: Opening the black box, *Anal. Chim. Acta.* **890** (2015) 60. doi: <https://doi.org/10.1016/j.aca.2015.07.030>
34. Gawkowska, D., Cieřla, J., Zdunek, A., Cybulska, J., Cross-linking of diluted alkali-soluble pectin from apple (*Malus domestica* fruit) in different acid-base conditions, *Food Hydrocoll.* **92** (2019) 285. doi: <https://doi.org/10.1016/j.foodhyd.2019.02.010>
35. Paudyal, H., Pangen, B., Inoue, K., Kawakita, H., Ohto, K., Ghimire, K. N., Alam, S., Adsorptive removal of trace concentration of fluoride ion from water by using dried orange juice residue, *Chem. Eng. J.* **223** (2013) 844. doi: <https://doi.org/10.1016/j.cej.2013.03.055>
36. Zong, E., Wei, D., Wan, H., Zheng, S., Xu, Z., Zhu, D., Adsorptive removal of phosphate ions from aqueous solution using zirconia-functionalized graphite oxide, *Chem. Eng. J.* **221** (2013) 193. doi: <https://doi.org/10.1016/j.cej.2013.01.088>
37. Ansari, A., Daigavane, P. B., Analysis and modelling of slope failures in municipal solid waste dumps and landfills: A review, *Nat. Environ. Pollut. Technol.* **20**(2) (2021) 825. doi: <https://doi.org/10.46488/NEPT.2021.v20i02.045>
38. Wang, R., Liang, R., Dai, T., Chen, J., Shuai, X., Liu, C., Pectin-based adsorbents for heavy metal ions: A review, *Trends Food Sci. Technol.* **91** (2019) 319. doi: <https://doi.org/10.1016/j.tifs.2019.07.033>
39. Nguyen, T. A. H., Ngo, H. H., Guo, W. S., Zhou, J. L., Wang, J., Liang, H., Li, G., Phosphorous elimination from aqueous solutions using zirconium loaded okara as adsorbent, *Bioresour. Technol.* **170** (2014) 30. doi: <https://doi.org/10.1016/j.biortech.2014.07.069>
40. Xu, J., Luu, L., Tang, Y., Phosphate removal using aluminium doped magnetic nanoparticles, *Desalin. Water Treat.* **58** (2017) 239. doi: <https://doi.org/10.5004/dwt.2017.0356>
41. Köse, T. E., Kivanç, B., Biosorption of phosphate from aqueous solutions using calcined waste eggshell, *Chem. Eng. J.* **178** (2011) 34. doi: <https://doi.org/10.1016/j.cej.2011.09.129>
42. Zhang, L., Wan, L., Chang, N., Liu, J., Duan, C., Zhou, Q., Wang, X., Removal of phosphate from water by activated carbon fiber loaded with lanthanum oxide, *J. Hazard. Mater.* **190** (2011) 848. doi: <https://doi.org/10.1016/j.jhazmat.2011.04.021>
43. Rai, R., Aryal, R. L., Paudyal, H., Gautam, S. K., Ghimire, K. N., Pokhrel, M. R., Poudel, B. R., Acid-treated pomegranate peel; An efficient biosorbent for the excision of hexavalent chromium from wastewater, *Heliyon.* **9**(5) (2023) e15698. doi: <https://doi.org/10.1016/j.heliyon.2023.e15698>
44. Ismail, Z. Z., Kinetic study for phosphate removal from water by recycled date-palm wastes as agricultural by-products, *Int. J. Environ. Stud.* **69**(1) (2012) 135. doi: <https://doi.org/10.1080/00207233.2012.656975>
45. Riahi, K., Thayer, B. B., Mammou, A. B., Ammar, A. B., Jaafoura, M. H., Biosorption characteristics of phosphate from aqueous solution onto *Phoenix dactylifera* date palm fibres, *J. Hazard. Mater.* **170** (2009) 511. doi: <https://doi.org/10.1016/j.jhazmat.2009.05.004>